ELSEVIER

Journal of Alloys and Compounds 293–295 (1999) 637–642

Journal of ALLOYS AND COMPOUNDS

Influence of cobalt content in $MmNi_{4.3-x}Mn_{0.3}Al_{0.4}Co_x$ alloy ($x=0.36$ and 0.69) on its electrochemical behaviour studied by in situ neutron diffraction

M. Latroche[a,*], A. Percheron-Guégan[a], Y. Chabre[b]

[a]*Laboratoire de Chimie Métallurgique des Terres Rares, CNRS, UPR 209, 2–8 rue Henri Dunant, 94320 Thiais Cedex, France*
[b]*Laboratoire de Spectrométrie Physique, Université J. Fourier–Grenoble, CNRS, BP 87, 38402 Saint Martin d'Hères, France*

Abstract

Ni–MH batteries have been widely studied and improved in recent years. Most of the negative electrodes of such batteries are made from $LaNi_5$-type alloys and improved materials have been obtained from pseudo-binary phases such as $MmNi_{3.55}Mn_{0.4}Al_{0.3}Co_{0.75}$. The advantage of cobalt addition has been demonstrated in terms of life-cycle improvement and corrosion resistance. However, cobalt remains the most costly element of the alloy. The behaviour of two electrodes with different cobalt amounts (5 and 10 wt.%) has been investigated by in situ neutron powder diffraction. The appearance of an intermediate γ phase during the charge process in the 10 wt.% Co alloy is observed and its role in the electrochemical process described. Crystallographic, electrochemical and kinetic behaviour of these electrodes are discussed in relation to cobalt concentration.

Keywords: Intermetallic alloys; Hydrides; Electrode material; Neutron diffraction

1. Introduction

Ni–MH batteries have been widely studied in the recent years since they are able to replace Ni–Cd ones in the large market of portable goods and electric vehicles. Most of the negative electrodes of such batteries are made of $LaNi_5$-type alloys [1,2] and improved materials have been obtained from complex pseudo-binary phases such as $MmNi_{3.55}Mn_{0.4}Al_{0.3}Co_{0.75}$ [3,4]. Though lanthanum has been replaced by cheaper mischmetal (Mm), alloy cost is still high especially with cobalt which represents only 10% in weight but 45% of the total alloy price. However, the interest of cobalt addition has been demonstrated in the past [5] and recent studies have shown that it plays an essential role in the improvement of life-cycle without significant capacity loss [6,7]. A powerful investigation of these material electrodes can be achieved by in situ neutron diffraction. This technique has been already successfully used on single- and multi-substituted compounds [8]. In this paper, it was shown that the pressure–composition isotherm (PCI) shape is very important for the life-cycle of such electrodes. Better results obtained for the compound $LaNi_{3.55}Mn_{0.4}Al_{0.3}Co_{0.75}$ were attributed to the existence of the large domain of the β branch (i.e. solid solution domain) where the volume expansion gradually increases in comparison to the equilibrium plateau process involving a discrete $\Delta V/V$.

In this paper, we present the results obtained by in situ neutron powder diffraction on two mischmetal electrodes with two different cobalt concentrations (5 and 10 wt.%). Crystallographic, electrochemical and kinetic behaviour of these electrodes are analysed and compared in relation to the amount of cobalt.

2. Experimental details

Both compounds were industrial samples. Stoichiometry and homogeneity were controlled both by metallographic examination and microprobe analysis. X-ray diffraction patterns were recorded on a Philips PW1710 goniometer using Cu Kα radiation. X-ray patterns were indexed in the $CaCu_5$ hexagonal cell ($P6/mmm$ space group) previously described for $LaNi_5$ [9,10]. Results of the characterisation are compiled in Table 1.

As neutron diffraction experiments need the use of deuterium instead of hydrogen which induces large incoherent scattering, PCI diagrams were characterised with D_2

*Corresponding author.

0925-8388/99/$ – see front matter
PII: S0925-8388(99)00357-6

Table 1
Characterisation of the electrode materials by electron probe micro-analysis (EPMA) and X-ray powder diffraction (XRD) (Number in brackets corresponds to the esd values)

Compound (Co wt%)	Microprobe analysis (±0.01)	Cell parameters (Å)		Cell volume V (Å^3)
		a	c	
5	$La_{0.52}Ce_{0.23}Nd_{0.22}Pr_{0.02}Ni_{4.00}Mn_{0.31}Al_{0.39}Co_{0.36}$	5.011(1)	4.052(1)	88.11(6)
10	$La_{0.51}Ce_{0.24}Nd_{0.23}Pr_{0.02}Ni_{3.61}Mn_{0.30}Al_{0.39}Co_{0.69}$	5.017(1)	4.048(1)	88.24(6)

gas in order to detect any isotopic effects. About 0.5 g of samples were ground mechanically under controlled atmosphere and activated by performing five solid–gas cycles. Then the desorption isotherm curves were determined by pressure variation measurements using calibrated and thermostated volumes.

Neutron diffraction experiments were performed at room temperature and atmospheric pressure on the D1B instrument at the Institut Laue Langevin in Grenoble. Wavelength was set to 2.523 Å and the patterns were recorded every 5 min for the 5% Co and every 20 min for the 10% Co with a position sensitive detector in the range $28° < 2\theta < 108°$ in step of 0.2°. The electrochemical neutron diffraction cell has been previously described [11]. The composite electrodes were made from about 14 g of alloy and were prepared as reported previously [8]. The electrodes were immersed in NaOD 5.5 N electrolyte which presents the same ionic conductivity as KOH 9 N used in commercial batteries but with a much lower viscosity allowing a continuous evolving of the produced bubbles. The potential was monitored against a $Cd/Cd(OH)_2$ reference electrode. The electrochemical process was driven with a microprocessor-controlled potentiostat–galvanostat MacPile from Biologic [12]. Before starting the in situ experiments, both electrodes were galvanostatically activated by cycling several times at $C/10$ for 15 h and $D/10$ with a cut off at 0.3 V vs. $Cd/Cd(OH)_2$ (see caption of Table 2 for the meaning of C/n or D/n). At the end of the last ex situ galvanostatic discharge, a complementary potentiostatic discharge was performed at 0.3 V in order to completely discharge each electrode and get its nominal capacity. These capacities were found in good agreement with the expected ones. Then a full charge was performed before starting the in-beam study of the 5%Co sample. The protocol for both electrodes is detailed in Table 2. Diffraction patterns have been analysed using the FULLPROF program [13].

3. Results

3.1. Isotherm curves

The PCI desorption curves at 25°C are shown in Fig. 1 for the two alloys. Maximum capacity and desorption equilibrium pressures are reported in Table 2. Both alloys exhibit rather sloped plateaus between 0.01 and 0.1 bar which is the suitable range for electrochemical applications. The expected capacities deduced from these solid–gas measurements and converted into electrochemical units are close to 300 mA h g^{-1} for both samples and are in good agreement with the measured ones.

3.2. Neutron diffraction

3.2.1. 5% Co sample

The behaviour of the electrode with 5% of cobalt is reported in Fig. 2. In the upper part of Fig. 2a, the respective amounts of each involved phase (α and β) is shown together with the total quantity of Coulomb Q

Table 2
Parameters of the experiment for the two electrodes[a]

Co (wt.%)	P_{des} (bar)	Cap. S.G. $P_{eq}=1$ bar D mol^{-1} (mA h g^{-1})	Active weight (g)	Activation ex situ	Nominal capacity after $Dp(0.3)$ (mA h g^{-1})	Electrochemical protocol in situ
5	0.11	4.75 (301)	13.87	Three charge–discharge cycles ($C/10$–$D/10$) + $Dp(0.3) + C/10$	304	$D/10$–R–$C/10$
10	0.06	4.50 (287)	14.66	Five charge–discharge ($C/10$–$D/10$) cycles + $Dp(0.3)$	290	$C/10 + C/7 + C/5$–R–$D/15 + R + Dp(0.1) + Dp(0.3)$

[a] The solid–gas (SG) capacity is measured under 1 bar of deuterium gas and converted into electrochemical units (mA h g^{-1}). The discharge electrochemical capacity is measured after several activation cycles. For electrochemical protocol, C/n (D/n) stands for nominal capacity galvanostatically charged (discharged) in n hours. $Dp(e)$ means a potentiostatic discharge at constant potential e (in V) vs. a $Cd/Cd(OH)_2$ reference electrode and R corresponds to an open circuit relaxation.

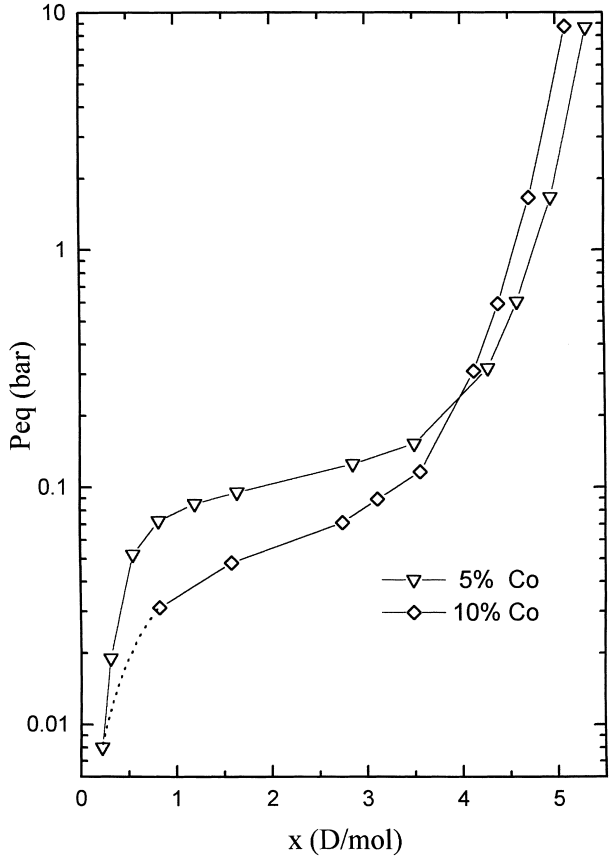

Fig. 1. Solid–gas (D_2) desorption PCI curves at room temperature for 5wt.% (▽) and 10 wt.% (◇) Co-containing alloys.

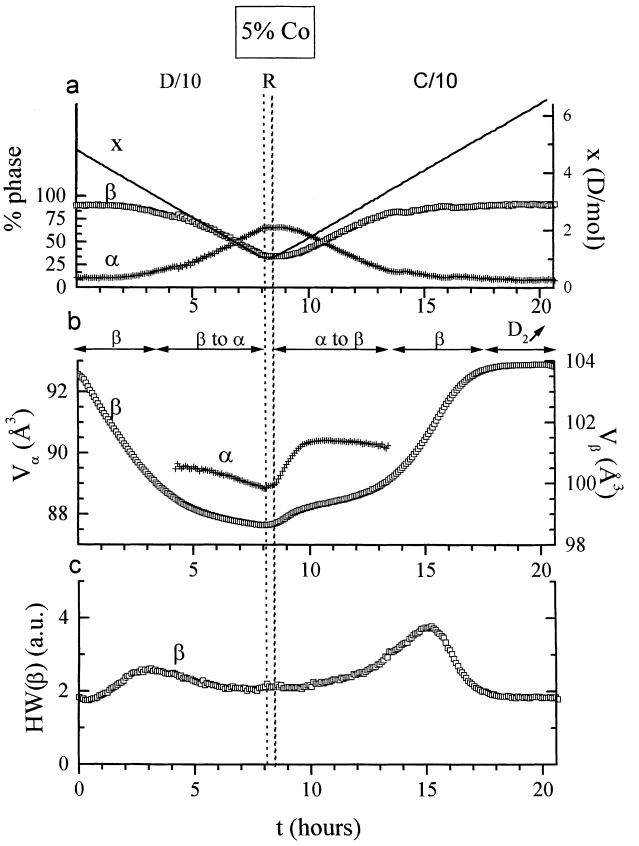

Fig. 2. Electrochemical cycling of the 5 wt.% Co electrode from a fully charged initial state: (a) intensities of the α (+) and β (□) phases (left axis) and measured capacity *x* (full line) determined from coulometric measurements (right axis). The % phase scale has been adjusted in order to get parallel slopes for the time dependence of both *x* and β lines. Note that *x* is not the real capacity of the hydride phase but corresponds to the quantity of Coulomb going through the electrode and converted in equivalent deuterium capacity. (b) Cell volume *V* of the α (+; left axis) and β (□; right axis) phases. (c) Evolution of the half width of the β (□) phase.

involved in the reaction, measured in mA h g^{-1} and converted in composition (*x* in D mol^{-1}) on the right hand scale. It is well known that during charge, gas evolving (i.e. D_2 formation) occurs at the surface of the negative electrode. Therefore, during charge the quantity of Coulomb as measured from *Q* is always larger than the state of charge of the electrode which explains the large values given on the right hand scale.

For one third of the discharge at *D*/10, the respective amounts of each phase are nearly constant meaning that the electrode works in the solid solution domain of the β branch. After 3 h, transformation of the deuteride into α phase is observed from line intensity variations, indicating that the system has reached the equilibrium plateau pressure. But it is only after 5 h that one has enough amount of this α phase to determine accurately its structural parameters. After 8 h, the discharge stops due to cut-off at 0.3 V although there is still some remaining β phase. The *C*/10 charge was then started after half an hour of open circuit relaxation and opposite effects take place. From the time of entering and leaving the two phase domain (at $t>3.5$ and $t<13.5$ h) one can estimate that the D content of the β phase is about 3.2 D mol^{-1}.

These limits also appear in the unit cell volume variations of both phases (Fig. 2b): large variations of the β volume are observed at the beginning of the discharge and at the end of the charge which corresponds to a solid solution behaviour whereas these volume variations are much smaller in the two phase domain. The end of charge ($t>17$h) with neither volume evolution nor relative phase amount changes corresponds to D_2 gas evolving. The cell volume jump observed at the beginning of the charge is connected with the volume gap for each phase (related to the hysteresis effect) between the absorption and desorption branches of the plateau pressure. Such a phenomenon has been already described earlier [8]. Beside, in agreement with the large volume change of the β phase in the solid solution domain, an important increase of the line width is observed at mid composition for this phase (Fig. 2c).

3.2.2. 10% Co sample

The results of the charge concerning the sample with 10% of Co are plotted on Fig. 3. During the first 2 h of the

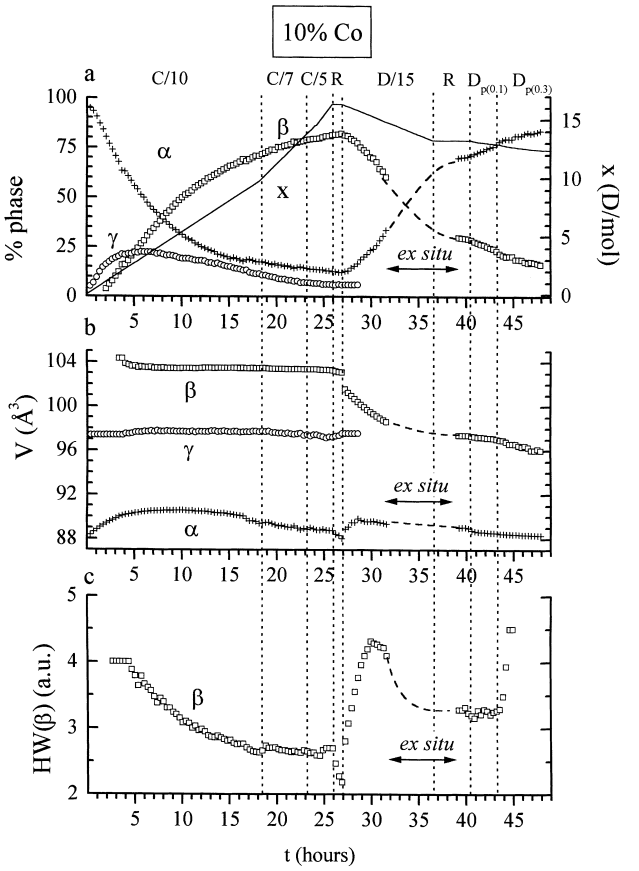

Fig. 3. Electrochemical cycling of the 10 wt.% Co electrode from a fully discharged initial state: (a) intensities of the α (+), γ (○) and β (□) phases (left axis) and expected capacity *x* (full line) determined from coulometric measurements (right axis). Note that *x* is not the real capacity of the hydride phase but corresponds to the quantity of Coulomb going through the electrode and converted in equivalent deuterium capacity. (b) Cell volume *V* of the α (+), γ (○) and β (□) phases. (c) Evolution of the half width of the β (□) phase.

charge, a classical two phase behaviour is observed. The amount of α decreases rapidly whereas the hydride phase appears. However, beyond this point, important differences with the 5% one are noticed. New diffraction lines are observed (see, for example, the one at $2\theta = 70.4°$ in the insert of Fig. 4a) and at this stage, it was necessary to account for a third phase to get a good refinement of the diffraction patterns. The results of these refinements let us conclude to the presence of the expected α ($V \approx 88–90$ Å^3) and β phases ($V \approx 103–104$ Å^3) plus an intermediate deuteride with V≈97–98 Å^3 that we called the γ phase. The amount of this γ phase goes through a maximum of 22 wt.% after 6 h of charge and then decreases to 5% at the end of the charge. In the mean time, the β phase amount increases up to 82 wt.% while the α phase correspondingly disappears.

It is worth noting that increasing the charge rates to *C*/7 and *C*/5, which means that the electrode was overcharged by a factor of about 3 (equivalent to $x \approx 15$ D mol^{-1} from converted electrochemical units) does not improve the charge kinetics and it was not possible to fully transform the α and γ phases into the β one. It is also interesting to notice that contrary to the 5% Co sample, the cell volumes of β and γ phases remain nearly constant during the whole process (Fig. 3b). In the same way, the half-width of the β phase (Fig. 3c) decreases continuously with a final drop at $t = 26$ h which corresponds to equilibration in the open circuit relaxation period after the end of the charge.

After this relaxation, a galvanostatic discharge at *D*/15 was started. Contrary to the charge, we observed a rapid decrease of the β phase volume from 103 to 99 Å^3 within 4 h. During the discharge, the lines corresponding to the γ phase rapidly merged with those of the β one and could not be observed anymore (see insert to Fig. 4b). Then, the data refinement involved only two phases: the β and α ones. Similarly, as observed for the 5% Co, a maximum in the half-width parameter is also observed at $t = 30$ h for the mid composition of the β branch.

4. Discussion

For the 5% Co sample, the electrode behaviour can be explained both from an equilibrium domain between the α and the β phases and a solid solution domain for the β one. In the two phase domain, phase percentages vary whereas the cell volumes remain constant. In the solid solution region, the relative amounts of each phase are unchanged when the β cell volume varies. At the end of the charge, D_2 gas evolving is clearly seen since the quantity of Coulomb *x* continues to increase whereas both cell volumes and phase amounts remain constant. Some remaining α phase attributed to non reacting part of the sample is also observed. The half width maximum observed for the pure β phase is attributed to the large gradient of composition within the grains in the β branch due to the electrochemical over-pressure at the grain surface. After the relaxation time in open circuit, the deuterium atoms diffuse within the grain and the instrumental line width is recovered.

For the 10% Co sample, from the diffraction pattern analysis it is first observed that there is coexistence of two deuterides during the charge process. Such a case has been already reported for other systems such as $LaNi_5$–H_2 [14,15]. There is no evidence neither for volume changes nor for half width maximum for these phases and therefore, it is concluded that during the charge there is no solid solution domains but only phase transformations. However, there is coexistence of three phases (α, β and γ), whereas from a thermodynamical point of view, we should observe only two phases corresponding first to the α↔γ plateau followed by the γ↔β one. One can consider that the *C*/10 experiment is an out of equilibrium process and that it can explain the coexistence of the three phases. From very careful electrochemical and solid–gas measure-

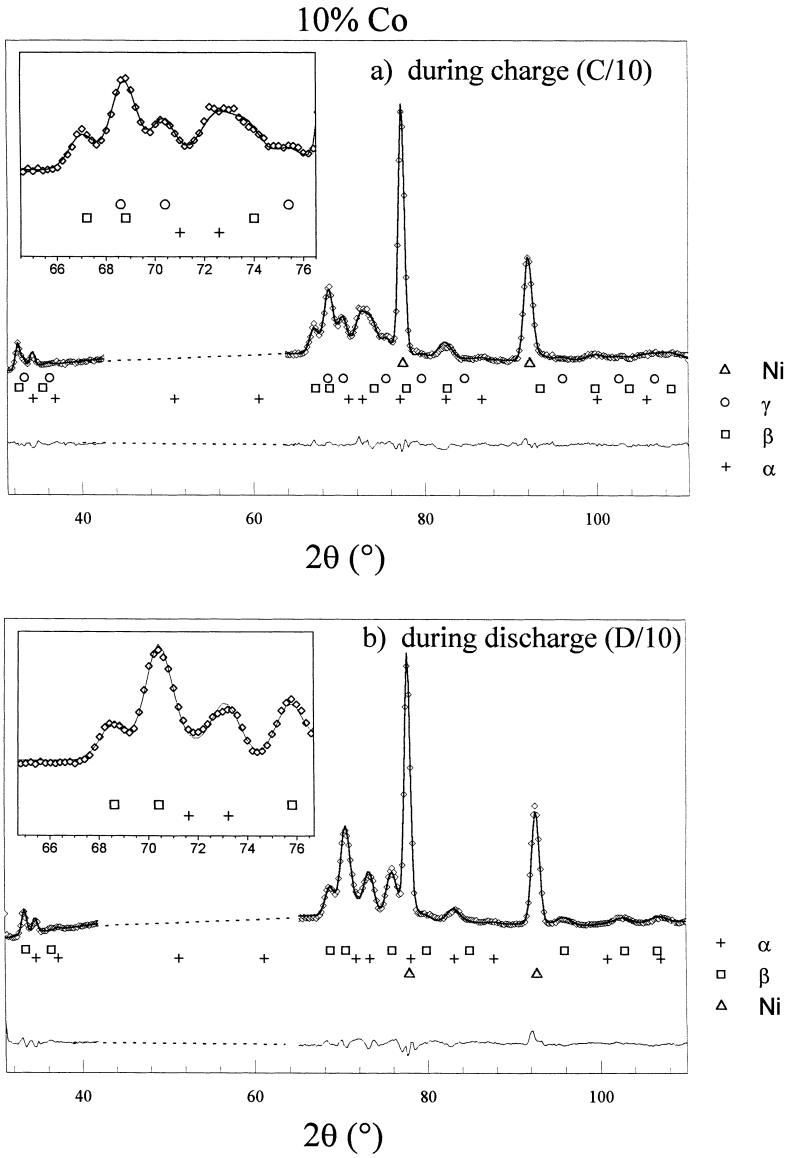

Fig. 4. Refined neutron diffraction pattern of the 10 wt.% Co alloy. (a) After 9 h of charge at $C/10$, (b) after 5 h of discharge at $D/15$, showing the experimental, calculated and difference curves. The range between $42° < 2\theta < 65°$ was excluded from the refinement due to the large background contribution induced by the electrolyte and the silica cell. The inset shows the detailed contribution between $64° < 2\theta < 77°$ involving three phases during the charge and only two phases for the discharge. Ni lines come from both the collector grid and the counter electrode.

ments performed at very low rates close to equilibrium, we were not able to observe a multiplateau behavior with an intermediate deuteride as it is clearly observed for the neighbouring system $LaNi_{5-z}Co_z$ [16]. Therefore, it is concluded that the γ phase is a metastable one. Such a behaviour has already been reported for of the intermediate hydride phase observed in the system $LaNi_5$–H_2 [14,15]. This hypothesis is supported by the fact that this phase is not observed in the discharge process and is therefore non-reversible within the hysteresis loop. This metastable phase is only formed during the charge. It is expected to exist at the interface between the α and the β phases and to propagate toward the core of the grains. It is worth noting that this intermediate phase was not observed for $LaNi_{3.55}Mn_{0.4}Al_{0.3}Co_{0.75}$ [8] and it seems to exist only with mischmetal and 10 wt% Co.

This γ phase with its intermediate cell volume (97–98 $Å^3$) plays probably a very important role in the strain distribution within the grain. The interesting feature of such a process is related to volume expansion. It is known that the large cell volume increase during the α to β transformation induces large decrepitation creating new fresh interfaces with the electrolyte and increasing corrosion [5]. An intermediate deuteride implies a two step process in the discrete volume expansion ($\alpha \rightarrow \gamma$, $\gamma \rightarrow \beta$) allowing the system to reduce the strains and therefore to limit the decrepitation process. This consideration is supported by scanning electron microscopy (SEM) ob-

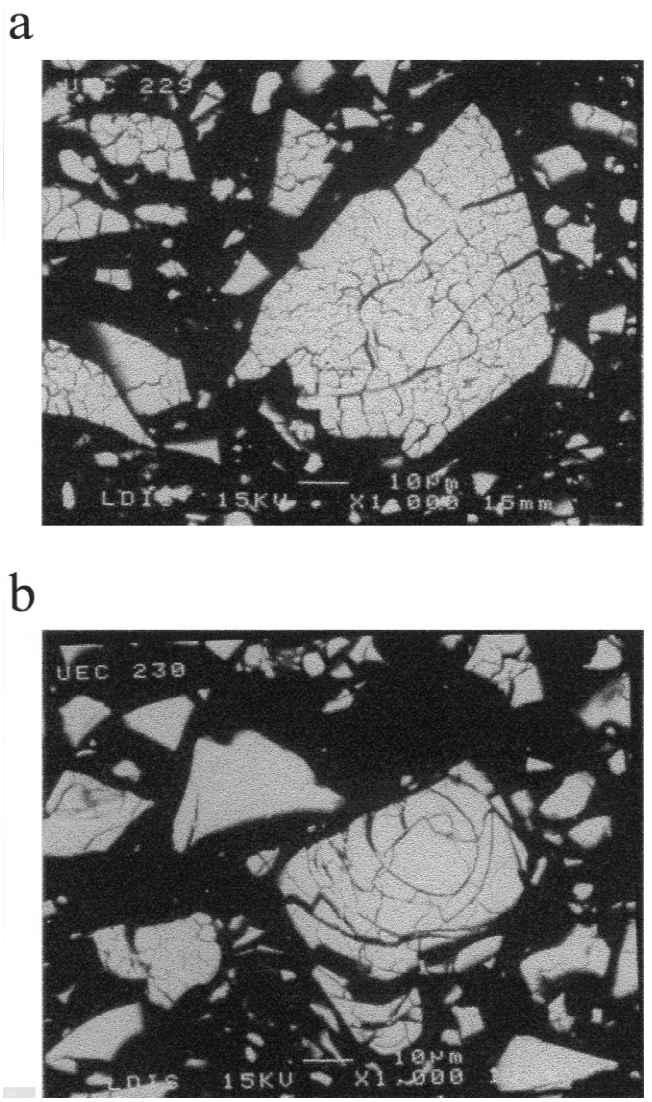

Fig. 5. Scanning electron microscope photographs of: (a) 5 wt.% Co, (b) 10 wt.% Co showing the decrepitation of the grains after electrochemical cycling.

servations performed on both 5% Co and 10% Co electrode materials after electrochemical cycling as shown on the pictures of Fig. 5.

5. Conclusion

The improved life-cycle for the Co-rich mischmetal sample is related to the presence of an intermediate γ phase deuteride, observed for the first time. This phase is metastable and is observed out of equilibrium during the charge process only, using in situ investigations. This intermediate deuteride involves a two-step process in the α to β transformation and it allows a reduction in the decrepitation induced by large volume expansion during the charge–discharge cycles and the subsequent sensitivity to corrosion.

Acknowledgements

We are thankful to B. Oulladiaf from the ILL for his help during the D1B experiment at the ILL in Grenoble.

References

[1] A. Percheron-Guégan, J.C. Achard, J. Sarradin, G. Bronoël, Electrode material based on lanthanum and nickel, electrochemical uses of such materials, French patents 75 16160 (1975), 77 23812 (1977); US patent 688537 (1978).
[2] J. Bouet, B. Knosp, A. Percheron-Guégan, J.M. Cociantelli, Matériau Hydrurable pour Electrode Négative d'Accumulateur Nickel–Hydrure, French patent 92 14662 (1992).
[3] H. Ogawa, M. Ikoma, H. Kawano, I. Matsumoto, Power Sources 12 (1988) 393.
[4] M. Ikoma, H. Kawano, I. Matsumoto, N. Yanagihara, Eur. Patent Appl. No. 0 271 043 (1987).
[5] J.J.G. Willems, Philips J. Res. 39 (Suppl. 1) (1984) 1.
[6] J.M. Cocciantelli, P. Bernard, S. Fernandez, J. Atkin, J. Alloys Compd. 253–254 (1997) 642–647.
[7] G.D. Adzic, J.R. Johnson, S. Mukerjee, J. McBreen, J.J. Reilly, J. Alloys Compd. 253–254 (1997) 579–582.
[8] M. Latroche, A. Percheron-Guégan, Y. Chabre, J. Bouet, J. Pannetier, E. Ressouche, J. Alloys Compd. 231 (1995) 537–545.
[9] A. Furrer, P. Fischer, W. Hälg, L. Schlapbach, Proc. Int. Symp. on Hydrides for Energy Storage 1977 (1978) 73.
[10] H. Nowotny, Zeitschrift für Metallkunde 34 (1942) 247.
[11] M. Latroche, A. Percheron-Guégan, Y. Chabre, C. Poinsignon, J. Pannetier, J. Alloys Compd. 189 (1992) 59–65.
[12] C. Mouget, Y. Chabre, Multichannel Potentiostatic and Galvanostatic System MacPile, licensed from CNRS and UJF–Grenoble to Bio-Logic Corp., 1 Ave. de l'Europe, F-38640 Claix.
[13] J. Rodríguez-Carvajal (Ed.), Abstracts of Satellite Meeting on Powder Diffraction, Cong. Int. Union Crystallogr, Toulouse, France, 1990, p. 127.
[14] T. Matsumoto, A. Matsushita, J. Less-Common Met. 123 (1986) 135–144.
[15] E. Akiba, K. Nomura, S. Ono, J. Less-Common Met. 129 (1987) 159–164.
[16] H.H. Van Mal, K.H.J. Buschow, F.A. Kuijpers, J. Less-Common Met. 32 (1973) 289–296.